HAL
open science

The effect of adsorbed oxygen species on carbon-resistance of Ni-Zr catalyst modified by Al and Mn for dry reforming of methane

Ye Wang, Li Li, Patrick Da. Costa, Changwei Hu, Chaojun Cui

To cite this version:

Ye Wang, Li Li, Patrick Da. Costa, Changwei Hu, Chaojun Cui. The effect of adsorbed oxygen species on carbon-resistance of Ni-Zr catalyst modified by Al and Mn for dry reforming of methane. Catalysis Today, 2021, 10.1016/j.cattod.2021.03.004 . hal-03167541

HAL Id: hal-03167541

https://hal.sorbonne-universite.fr/hal-03167541

Submitted on 12 Mar 2021

HAL is a multi-disciplinary open access archive for the deposit and dissemination of scientific research documents, whether they are published or not. The documents may come from teaching and research institutions in France or abroad, or from public or private research centers.

L'archive ouverte pluridisciplinaire **HAL**, est destinée au dépôt et à la diffusion de documents scientifiques de niveau recherche, publiés ou non, émanant des établissements d'enseignement et de recherche français ou étrangers, des laboratoires publics ou privés.

The effect of adsorbed oxygen species on carbon-resistance of Ni-Zr catalyst modified by Al and Mn for dry reforming of methane

Ye Wang [a, b], Li Li [c], Chaojun Cui [a], Patrick Da. Costa [b, *] and Changwei Hu [a, c, *]

a: College of Chemical Engineering, Sichuan University, Chengdu, Sichuan 610065, P. R. China

b: Sorbonne Université, Institut Jean Le Rond d'Alembert, CNRS, 2 Place de la Gare de Ceinture, Saint-Cyr-L'Ecole 78210, France

c: Key Laboratory of Green Chemistry and Technology, Ministry of Education, College of Chemistry, Sichuan University, Chengdu, Sichuan, 610064, P. R. China

E-mail: patrick.da_costa@upmc.fr (P. Da Costa) and changweihu@scu.edu.cn. (C. Hu)

Abstract:

Dry reforming of methane was investigated over Ni-Zr catalysts modified by Aluminum and Manganese. The catalysts were characterized by XRD, CO_2-TPD, XPS, TGA, and Raman. Among all prepared catalysts, the 5Al-5Mn (5 wt% Al and 5 wt% Mn) catalyst showed the highest CH_4 and CO_2 conversion at 700 ^{o}C DRM with low carbon deposition. The CO_2-TPD results exhibited that the 5Al-5Mn catalyst had the highest amounts of both total basic sites and medium-strength basic sites, which could promote the adsorption and activation of CO_2 molecule during the DRM reaction, and further reduce the carbon deposition. The XRD results suggested that the addition of both Al and Mn led to smaller nickel particle size. Besides, the lower carbon deposition on 5Al-5Mn and 2.5Al-7.5Mn catalyst was derived from a higher content of surface adsorption oxygen species, which was verified by the O 1s results. While the lower number of basic sites, more strong basic sites and larger particle size on 5Mn and 5Al catalysts result in a higher amount of carbon deposition.

Keywords: Carbon resistance, Dry reforming of methane, Adsorbed oxygen species, Manganese, Aluminum

1. Introduction

Nowadays, there is a huge interest in topics focusing on alternative energy, global warming, and greenhouse gases. Because the limited oil reserves decrease rapidly, other renewable sources need to be exploited [1]. Dry reforming of methane (DRM) offers an interesting opportunity to address these problems since it can utilize marsh gas and biomass pyrolysis gas directly [2, 3]. The nickel is the most appropriate catalyst for DRM due to high activity and low-cost [4-6]. However, Ni-based catalysts are suffered from deactivation through the sintering of metal and carbon deposition [4, 7]. So, a lot of studies have been investigated in the carbon-resistant for DRM [8-14].

Generally, promoters are used in order to reduce the carbon deposition over nickel-based catalyst via the following mechanisms: i) promoters could increase the number of basic sites, which could promote the adsorption and/or activation of CO_2; ii) promoters could enhance the dispersion of nickel particles; iii) promoters could promote the formation of oxygen vacancies [15-21]. Pompeo [22] investigated the influence of α-Al_2O_3, ZrO_2, and α-Al_2O_3-ZrO_2 on the performance of catalysts. The author found that Ni/α-Al_2O_3-ZrO_2 showed higher stability for 700 ^oC DRM reaction, due to the lower coke formation on Ni/α-Al_2O_3-ZrO_2 catalyst; because both Al_2O_3 and ZrO_2 could increase the CO_2 adsorption and further decrease the carbon deposition. Wang et al. [23] studied Mn doping nanocrystalline Co–Ce–Zr–O_x catalysts for DRM reaction. The conversions of CO_2 and CH_4 were 74 % and 70 %, respectively. While the conversions of CO_2 and CH_4 were both lower than 40 % on non-promoted nanocrystalline Co–Ce–Zr–O_x catalyst. The promoted activity was attributed to the increasing availability of surface oxygen species and the better oxygen mobility on Mn-modified catalyst, as well as the better dispersed nano-sized Co_3O_4. Bellido et al. [24] prepared nickel supported on ZrO_2 stabilized with various content of Y_2O_3. The Ni/8Y_2O_3–ZrO_2 (with a Y_2O_3 load of 8 mol%) catalyst showed the best catalytic performance for DRM reaction with the initial CH_4 conversions of 72 %. The author found the interaction between the surface oxygen vacancies and nickel species on the Y_2O_3–ZrO_2 support enhanced by the increasing Y_2O_3 load, which could improve the CH_4 and CO_2 conversion in the dry reforming of methane reaction. Besides, according to the literature [15, 20], the surface oxygen vacancies could promote the elimination of coke, because the surface oxygen vacancies could induce oxygen radicals from the CO_2 to react with carbon deposition.

The promotion of Al resulted in higher activity for DRM due to the higher reducibility and dispersion of nickel, reported by Liu et al. [25]. Talkhoncheh et al. [26] analyzed the effect of clinoptilolite, ceria, and alumina supports on the activity for DRM. The Ni/Al_2O_3 catalyst exhibited the highest catalytic performance since the even distributions and high specific surface area. The addition of Mn can contribute to carbon removal with the sacrifice on the activity [27]. Yao et al. [28] and Seok et al. [29] also found that Mn promoter could reduce the carbon deposition by the smaller particle size of nickel species. The introduction of Al and Mn was conducive to the activation for DRM, reported by Li et al. [30].

Herein, we prepared Ni-Zr materials promoted by Mn and Al, which were applied to the dry reforming of methane. To understand the relationship between the carbon deposition and the surface structure of the catalysts, CO_2-TPD, XRD, XPS, TGA, and Raman were conducted.

2. Experiment

2.1 The preparation of catalysts

The catalysts are prepared via a one-step synthesis method route [31]. P123, $Ni(NO_3)_2{\cdot}6H_2O$, $ZrO(NO_3)_2{\cdot}xH_2O$, CH_4N_2O, and $Al(NO_3)_3{\cdot}9H_2O$ and/or $Mn(NO_3)_2{\cdot}4H_2O$ were dissolved in distilled water (375 mL). The molar loadings of Ni, Al, Zr, and Mn were listed in **Table 1**. The mixture of aqueous solutions was heated from room temperature to 95 °C under vigorous stirring for 48 h in air. Then this suspension was subsequently aged in an oven (100 °C) for 24 h in a closed vessel. Next, this slurry was suction filtered and washed by distilled water with equal volume of obtained materials for three times. The solids obtained were dried at room temperature. Finally, the precursor was calcined at 800 °C for 5 h with an increasing rate of 1 °C/min under airflow. The catalysts were denoted as 5Al, 7.5Al–2.5Mn, 5Al–5Mn, 2.5Al–7.5Mn, and 5Mn respectively.

Table 1 The molar loadings of Ni, Zr, Al, and Mn on a series of promoted Ni-Zr materials

Catalyst	Nickel %	Zirconium %	Aluminum %	Manganese %
5Al	10	85	5	-
7.5Al–2.5Mn	10	80	7.5	2.5
5Al–5Mn	10	80	5	5

2.5Al–7.5Mn	10	80	2.5	7.5
5Mn	10	85	-	5

2.2 The catalytic performance of catalysts

The DRM activity test was performed in a fixed-bed flow microreactor with a K-type thermocouple to monitor the temperature of the catalytic bed. At first, the catalysts were reduced at 750 °C under the 5 vol% H_2/Ar flow for one hour. And then, the surface of reduced catalysts was cleaned by argon flow. Last, the mixed gases were introduced to the catalyst bed. The ratio of CO_2: CH_4: Ar was 1: 1: 8, corresponding to a GHSV of 48,000 h^{-1}. The effluents were analyzed by using an online gas micro chromatography (490 Varian Micro-GC). The H_2/CO molar ratio and the conversions of CH_4 (X_{CH_4}) and CO_2 (X_{CO_2}) and were calculated as follows:

$$X_{CH_4} = \frac{n_{CH_4,in} - n_{CH_4,out}}{n_{CH_4,in}} \times 100\% \quad (1)$$

$$X_{CO_2} = \frac{n_{CO_2,in} - n_{CO_2,out}}{n_{CO_2,in}} \times 100\% \quad (2)$$

$$H_2/CO = n_{H_2,out}/n_{CO,out} \quad (3)$$

Where X_i and H_2/CO refers to the conversion of *i* species, and the molar ratio of H_2/CO. The $n_{j,in}$ is the number of moles of *j* species in feed gas. The $n_{j,in}$ is the number of moles of *j* species in out gas.

2.3 The characterization of catalysts

The CO_2-TPD experiments in the range of 80 to 900 °C were measured on a BELCAT-M measurement, equipped with a TCD. The fixed-bed reactor loaded with ca. 60 mg of sample, using a heating rate of 10 °C/min. After an *in-situ* reduction at 750 °C under a 5 % H_2/Ar flow, the sample was cooled down to 80 °C, introducing in a mixture flow of 10% CO_2/He for 60 min. Last, the desorption process was under a He flows with an increasing temperature (80 to 900 °C).

The powder XRD patterns were recorded on a DX-1000 CSC diffractometer with a Cu Kα radiation source. The voltage and current were 40 kV and 25 mA, respectively. The Bragg angles were recorded in the range of 10 ° < 2θ < 80 °, with 0.3 s $step^{-1}$ scan speed and 0.03 ° scan step size. The crystallite size on catalysts was calculated by using the Scherrer Equation.

The thermogravimetric analysis (TGA) was conducted on the NETZSCH STA 449F5 instrument.

The temperature of the sample was increased from 35 to 800 °C with a heating rate of 5 °C/min, and at the same time, the sample was oxidized by air flow (60 ml/min). The weight of the sample was recorded from 35 to 800 °C.

The X-ray photoelectron spectroscopy (XPS) was conducted on a KRATOS spectrometer with an AXIS Ultra DLD to detect the surface elements of catalysts.

Raman spectroscopy experiments were conducted on an objective (X50LWD) with a Grating of 600 gr/mm, a Laser of 532.17 nm, a Hole of 200 μm, and a Filter of D1. The data was collected from the wavenumber values of 1000−2000 cm^{-1}.

3. The results and discussion

3.1 Catalytic activity for CO_2 reforming of methane at medium temperature

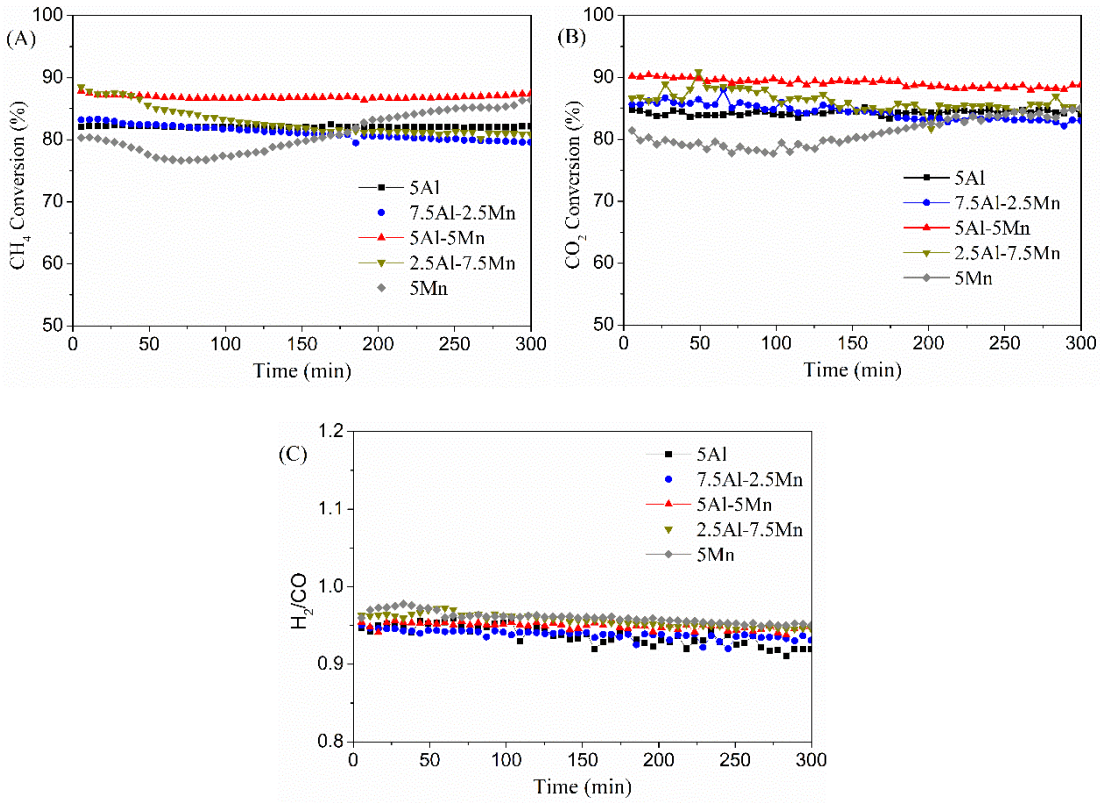

Figure 1 The conversion of CH_4 (A) and CO_2 (B), and (C) the rate of H_2/CO of the series of Al-Mn-Ni-Zr catalysts at 700 ^{o}C.

The effect of Al and/or Mn promoters was investigated in previous work [25, 28, 32, 33]. It was shown that the catalytic performance of Al-promoted catalysts was higher than that of non-promoted catalyst. Liu et al. [25] and He et al. [33] reported the introduction of Al results in

low Ni particle sizes, thereby enhancing the activity for DRM. The references [25, 28] reported that the Mn promoter could enhance the carbon-resistance of nickel-based catalysts with a decrease of catalytic activity. The Ni-Zr catalyst exhibited a decrease activity within 100 min, which was lower than 5Al-5Mn catalyst (Figure S1). Herein, the two promoters Al and Mn were combined for designing a novel type of Al-Mn promoted Ni-Zr catalyst to obtain a higher catalytic performance for DRM.

Ni-Zr catalysts modified by the various ratio of Al/Mn promoters were tested in DRM at 700 ^{o}C with GSHV of 48,000 h^{-1}, for 300 minutes of time-on-stream (TOS) with the mixed flow of CH_4: CO_2: Ar=1: 1: 8. The results of activity tests are presented in **Figure 1**, including both conversions of CH_4 and CO_2, and the molar ratio of H_2/CO for a series of Ni-Zr catalysts. All the series of Ni-Zr catalysts were found to be catalytically active for both CO_2 and CH_4 conversions (> 80 %) for the initial reaction time-on-stream. As given in **Table 2**, the initial methane conversion was 82.0 %, 83.2 %, 87.8 %, 88.5 % and 80.3 % respectively for 5Al, 7.5Al-2.5Mn, 5Al-5Mn, 2.5Al-7.5Mn and 5Mn. The CO_2 conversion followed the sequence: 90.2 for 5Al-5Mn > 86.6 % for 2.5Al-7.5Mn > 85.6 % for 7.5Al-2.5Mn > 83.8 % for 5Al > 81.4 for 5Mn. However, a little bit of difference appeared when the activity of the Ni-Zr catalysts was compared with time on stream. The CH_4 conversion increased with TOS on the 5Mn catalyst. A similar observation of increased activity was reported by Li et al. [34]. The author found that Mn improved the dispersion of nickel species and enhanced the interaction between nickel and support with TOS, and further enhanced the catalytic for DRM. While the CH_4 conversion decreased on other catalysts, especially on 2.5Al-7.5Mn, it decreased by 8.6 %. The relative changes in CH_4 conversion were not significant for the 5Al-5Mn catalyst, manifesting this was the most stable catalytic activity among the studied catalysts. A similar trend can be observed for the relative change in CO_2 conversion, i.e. -0.8, -3.9, -1.6, -2.0, and +4.8 for 5Al, 7.5Al-2.5Mn, 5Al-5Mn, 2.5Al-7.5Mn, and 5Mn catalysts, respectively.

Table 2 The initial and after 5h activity, and the relative change in activity.

	Initial conversion		5 h conversion		Δ: Relative change after 5 h	
Catalysts	CH_4 (%)	CO_2 (%)	CH_4 (%)	CO_2 (%)	CH_4 (%)	CO_2 (%)
5Al	82.0	84.7	81.0	84.0	-1.2	-0.8

7.5Al-2.5Mn	83.2	85.6	79.5	82.3	-4.5	-3.9
5Al-5Mn	87.8	90.2	87.4	88.7	-0.4	-1.6
2.5Al-7.5Mn	88.5	86.6	80.9	84.9	-8.6	-2.0
5Mn	80.3	81.4	86.5	85.3	+7.7	+4.8

Besides, the 5Mn catalyst presents the highest ratio of H_2/CO than the studied catalysts, as presented in **Figure 1** (C). The ranking in H_2/CO ratio is found as follows: 5Mn > 5Al-5Mn > 2.5Al-7.5Mn > 7.5Al-2.5Mn > 5Al. Side reactions such as the reverse water-shift reaction (RWGS) and the disproportionation of CO reaction could results in the lower than unity H_2/CO ratio [15, 20, 35]. The disproportionation of CO reaction ($2CO \rightarrow CO_2 + C$, $\Delta H = -172.4\ \mathrm{kJ/mol}$) is a highly exothermic reaction [36]. Thermodynamically, the reaction is favoured at low temperatures and high pressure. Besides, the RWGS reaction is thermodynamically favorable and rapid to reach equilibrium under the reaction temperature between 500 and 700 °C [37, 38]. Thus, both RWGS and the disproportionation of CO could give rise to the lower H_2/CO ratio at 700 °C. Besides, the CO_2 conversion is higher than the CH_4 conversion on all the catalysts. Meanwhile, the ratio of H_2/CO shows a decreasing trend on 5Al, 7.5Al-2.5Mn, 2.5Al-7.5Mn, and 5Mn catalysts, suggesting that the reverse water-shift reaction is promoted with TOS [30]. In the whole process, the 5Al-5Mn catalyst exhibited the highest activity and stability in the 5 h time on stream for dry reforming of methane.

3.2 Carbon deposition analysis

According to the literature, the promotion by Mn could lead to a decrease in the carbon deposition of Ni-based catalysts during the DRM reaction [25, 28, 29, 39]. Herein, the carbon deposition on spent catalysts was measured by TGA experiments (**Figure 2**). It is worth noting that a small weight increase is observed in the 200-400 ^{o}C range on all the catalysts, which is consistent with our previous work [31, 40], and resulted from Ni^0 oxidation to NiO. Then a weight decline is observed at 400-700 ^{o}C and arises from the removal of different types of carbon species. Thus, the carbon deposition on spend catalysts was 2.5 %, 3.6 %, 6.3 %, 11.1 % and 14.0 % on 2.5Al-7.5Mn, 5Al-5Mn, 5Mn, 7.5Al-2.5Mn and 5Al catalysts, respectively. Both Al and Mn promoted catalysts

exhibited lower carbon deposition, indicating that the promotion of both Al and Mn could reduce the carbon deposition in DRM. The 2.5Al-7.5Mn catalyst exhibited the lowest carbon deposition since the conversion of CH_4 decreases with time on stream, while the CO_2 conversion does not change. Thus, the higher CO_2 conversion related to parallel reactions taking place during the DRM reaction, which can promote carbon removal during DRM. Besides, the 7.5Al-2.5Mn catalyst displays behavior different from other catalysts containing Al. The decrease in weight starts at around 350 ^{o}C in comparison to other catalysts in which the start is around 450°C. Meanwhile, two peaks in the DSC curve can be observed at 350-700 ^{o}C on the 7.5Al-2.5Mn catalyst. All the DSC signals imply that both processes (the oxidation of Ni^0 species and the elimination of carbon species) have an exothermic character, which has been reported in the literature [40]. The best results for both activity and carbon deposition were obtained for the 5Al-5Mn catalyst.

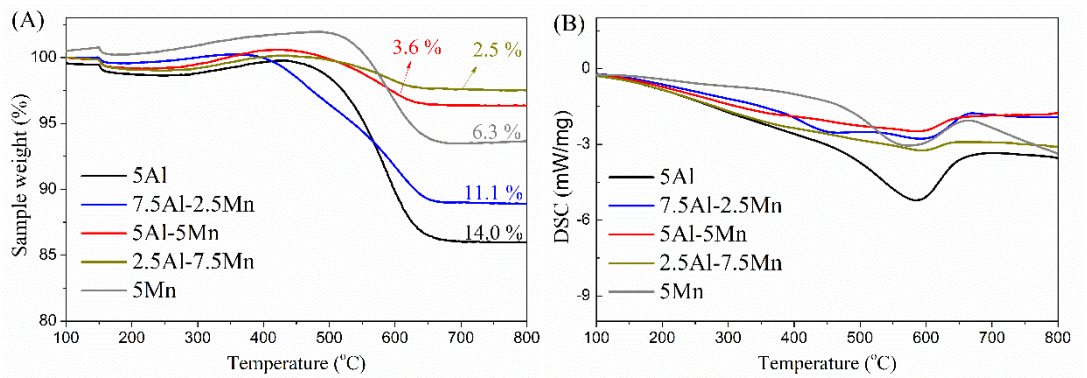

Figure 2 The TGA profiles of a series of used Al-Mn-Ni-Zr catalysts, (A) The sample weight curve and (B) the DSC curve.

In order to define the carbon species formed during DRM on the studied catalysts, Raman spectroscopy was performed. The results are reported in **Figure 3**. Two peaks at about 1350 and 1580 cm^{-1} could be observed on all spent Ni-Zr-Al-Mn catalysts, which can be assigned to the D band (from disorder) and G band (from graphite), respectively, as reported elsewhere [35, 41, 42]. The intensity of D (I_D) and G (I_G) band on both 5 Al-5Mn and 2.5Al-7.5Mn catalysts is weaker than that on others, which is in agreement with the TAG analyses. The D band results from the defective graphite unit cell, which is broken by an edge atom or a heteroatom [43]. The I_D and I_G are the peak area of D and G band in the curve of Raman, respectively. And the ratio of I_D/I_G is related to the parameter of defectiveness of carbon materials [44]. After 5 h (300 min) of the DRM

test, the 7.5Al-2.5Mn catalyst exhibits the highest I_D/I_G (1.0), others are 0.9, 0.8, 0.7, 0.5 for 5Al, 5Al-5Mn, 2.5Al-7.5Mn and 5Mn catalysts, respectively. These later results imply that the addition of Mn can decrease the ratio of I_D/I_G. According to the literature [28, 29], the addition of Mn as promoter can reduce the carbon deposition over Ni-based catalysts due to the smaller nickel particle size. Herein, the lower I_D/I_G ratio manifests that manganese also can promote the formation of graphite.

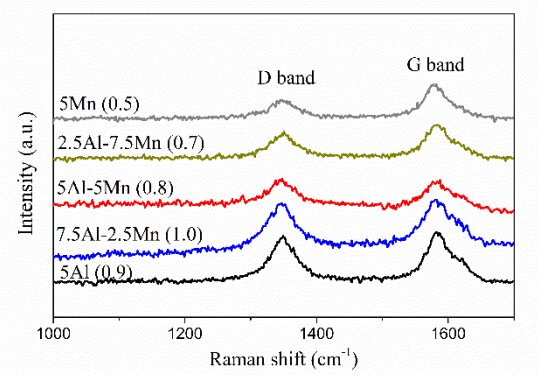

Figure 3 The Raman profiles of used Al-Mn-Ni-Zr catalysts

Besides, concerning the types of carbon deposition on 5Al and 5Mn catalysts. The decrease in weight over 5Al catalyst starts at around 450 °C (**Figure 2**), while it shifts to 530 ^{o}C on 5Mn catalyst, which might mean different types of carbon on 5Al and 5Mn catalyst. Besides, the DSC curve of 5Al catalyst exhibited a wide peak at 200 to 450 ^{o}C and a main peak at about 580 ^{o}C. Whereas for 5Mn catalyst, the DCS curve showed a very weak and wide peak at 350 to 450 ^{o}C and a main peak at 580 ^{o}C. According to the Raman results, the ratio of I_D/I_G is 0.9 and 0.5 on 5Al and 5Mn catalysts, respectively, indicating that more content of D band carbon formed on 5Al catalyst. In our previous work [35]. The D band carbon was easy to be removed. Thus, the carbon with higher content of D band on 5 Al catalyst was easy to be removed. Besides, this higher content of G band carbon on 5Mn catalyst presented the higher crystalline degree of the carbon materials [44], which was also verified by XRD results. The reflection of carbon could be detected on spent 5Mn catalyst with the crystallite size of 12 nm (Table 5). It is observed that the 5Al catalyst exhibits the highest carbon deposition of 14.0 %, which is higher than the used 5Mn catalyst (6.3 %). While the crystallite size of carbon deposition on the used 5Al catalyst (11 nm) is smaller than on the used 5Mn catalyst (12 nm). A lot of carbon on 5Mn catalyst is the graphene

carbon, which is accordance with the Raman results. Therefore, the 5Al and 5Mn catalysts exhibited two kinds of carbon (disorder and graphite) with different ratio of I_D/I_G.

3.3 Basicity, physical-chemical features, and surface characterization

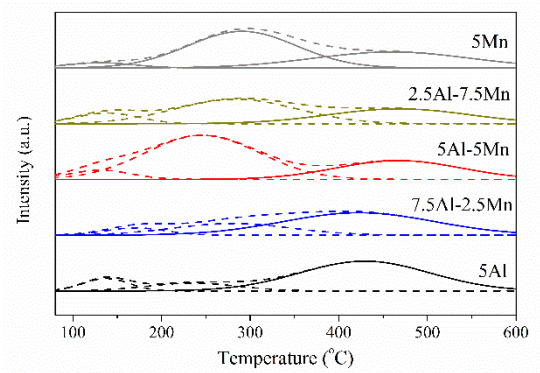

Figure 4 The CO_2-TPD profiles of Ni-Zr-Al-Mn catalysts in situ reduction at 750 °C

It is well known that basicity has a key role in the resistance against carbon formation in DRM since the carbon deposition derived from CH_4 decomposition is well-known to be deposited on the acid sites from the support [12]. Besides, the addition of basic promoters favors CO_2 adsorption and its dissociation, which contributes to the gasification of the carbon and thus to inhibiting the deactivation due to carbon formation [45-47]. Therefore, the lower concentration of basic sites might result in carbon deposition. CO_2-TPD was performed to evaluate the basicity of the studied catalysts; the results were presented in **Figure 4**. From CO_2-TPD plots, one can note that all Ni-Zr-Al-Mn catalysts present three typical CO_2 desorption peaks from 100 to 600 °C. First, one can note that the peaks in the CO_2-TPD curve on 5Mn, 2.5Al-7.5Mn, and 5Al-5Mn catalysts shift to low temperature compared to 7.5Al-2.5Mn and 5Al catalysts. This implies that the Mn promotion could lead to a decrease in the basicity of Ni-Zr-Al-Mn catalysts. Moreover, the total amount of basic sites varies differently. According to **Table 3**, the highest number of basic sites is obtained on the 5Al-5Mn catalyst (84 μmol CO_2/g), which is higher than Ni-Zr catalyst (73 μmol CO_2/g) [31]. The CO_2-TPD overall peak can be deconvoluted into three peaks corresponding to weak basic sites, medium-strength basic sites, and strong basic sites, which are mainly consisted

of weak Brønsted basic sites (surface OH groups), Lewis base sites (unsaturated (cus) O^{2-} and Zr^{4+}–O^{2-} centers), and the cus Zr^{4+} centers with strong Lewis acidity, respectively [45, 48]. In this study, the highest content of medium-strength basic sites is obtained on the 5Al-5Mn catalyst (52 μmol CO_2/g). The ranking in CO_2 desorbed with medium-strength is as follows: 46 μmol CO_2/g for 5Mn > 43 μmol CO_2/g for Ni-Zr [31] > 33 μmol CO_2/g for 2.5Al-7.5Mn > 9 μmol CO_2/g for both 7.5Al-2.5Mn and 5Al catalysts. The introduction of Mn leads to a decrease in the amount of CO_2 corresponding to strong basic sites compared to Al-promoted catalysts. The medium-strength basic sites could promote the adsorption and/or activation of CO_2, and further reduce the carbon deposition, as well as the deactivation of catalyst as it had already been reported in the literature [2, 49, 50].

Table 3 The CO_2-TPD profiles of Ni-Zr-Al-Mn catalysts in situ reduction at 750 ^oC

	CO_2 desorbed (μmol CO_2 /g)						
	Peak 1 weak		Peak 2 medium-strength		Peak 3 strong		
Catalyst	Position (^oC)	Content (%)	Position (^oC)	Content (%)	Position (^oC)	Content (%)	Total basicity (μmol CO_2/g)
5Al	134	7	231	9	435	47	63
7.5Al-2.5Mn	169	4	282	9	425	44	57
5Al-5Mn	129	8	248	52	469	24	84
2.5Al-7.5Mn	136	9	281	33	467	22	64
5Mn	133	7	288	46	474	24	77

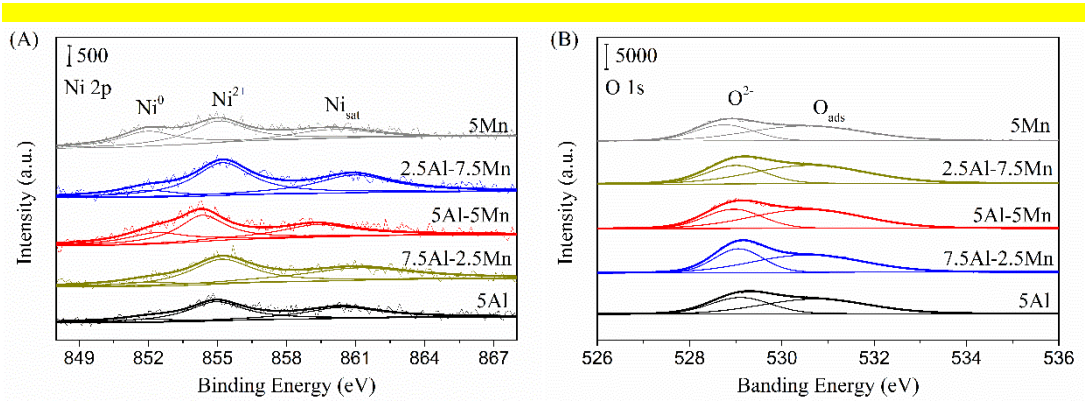

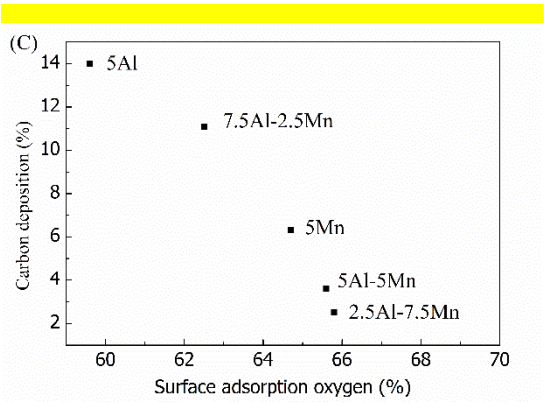

Figure 5 (A) The Ni 2p and (B) the O 1s profiles of Ni-Zr-Al-Mn catalysts after reduction, and (C) the relationship between the carbon deposition and the content of surface adsorbed oxygen species.

Table 4 presents the surface elemental content of reduced catalysts. The content of Ni species was 6.3, 6.8, 7.8, 8.9 and 8.6 % for 5Al, 7.5Al-2.5Mn, 5Al-5Mn, 2.5Al-7.5Mn, and 5Mn catalysts, respectively. It can be observed that the surface Ni content increased with the increase of Mn content when both Al and Mn promoters existed. It means the Mn enhance the enrichment of nickel species on the surface of catalyst. Besides, the Ni 2p curve (**Figure 5** (A)) was resolved to two peaks at about 852.3±0.5 eV, 854.5±0.5 eV with the corresponding satellite at about 861.0±0.5 eV, which were corresponded to Ni^0 and Ni^{2+} species, respectively [51] (Figure 5). The content of each peak was listed in **Table 4**. The 5Al-5Mn catalyst showed the higher Ni^0 content than other Al-containing catalyst. The Ni^0 species might promote both the dry reforming of methane and methane decomposition [52]. Thus, the 5Mn-5Al catalyst exhibited higher activity for DRM reaction. Although the 5Mn catalyst exhibited the highest content of Ni^0 species of 3.6 %, it showed the lowest activity in the beginning, which might be caused by the methane decomposition, especially 5Mn catalyst that contained Ni in considerable amounts. The carbon deposition on 5Mn catalyst may cause its partial deactivation. Thus, the activity decreased within first one hour. Similar results have been reported in the literature [53].

Table 4 The surface elemental content of 5Al, 7.5Al-2.5Mn, 5Al-5Mn, 2.5Al-7.5Mn, and 5Mn reduced catalysts.

	Ni	Zr	Al	Mn	O

	Total (%)	Ni^{0} (%)	Ni^{2+} (%)	(%)	(%)	(%)	(%)
5Al	6.3	0.9	5.4	53.6	5.1	-	35.0
7.5Al-2.5Mn	6.8	1.1	5.7	51.4	4.9	2.1	34.8
5Al-5Mn	7.8	2.9	4.9	50.4	4.1	4.8	32.9
2.5Al-7.5Mn	8.9	1.8	7.1	52.4	1.4	5.0	32.3
5Mn	8.6	3.6	5	46.7	-	6.5	38.2

In addition to the basicity of the catalysts, one of the important factors is the adsorption of surface oxygen species, which is known to promote the activation of CO_2, leading to the decrease of the carbon deposition and the enhancement in the stability of the catalyst for DRM reaction [31, 54]. **Figure 5** (B) shows the O 1s profiles from XPS spectroscopy (526 to 536 eV) of reduced studied catalysts. The peak at about 529 eV is assigned to the lattice oxygen species (O^{2-}), while another peak at 531 eV is attributed to the adsorbed oxygen species (O_{ads}) [31, 54-56]. The highest content of surface adsorbed oxygen species is obtained on 2.5Al-7.5Mn catalyst (65.8 %), which also corresponds to the lowest carbon deposition, as shown in **Figure 5** (C). One can also note from Figure 5 (B) that the content of O_{ads} species follows the sequence: 2.5Al-7.5Mn > 5Al-5Mn > 5Mn > 7.5Al-2.5Mn > 5Al. An opposite order in the carbon deposition can be observed on Ni-Zr-Al-Mn catalysts. This positive role of adsorbed oxygen species on ZrO_2 support has already been reported by Zhang et al. [54]. The author found the higher content of adsorbed oxygen species could contribute to the adsorption and activation of CO_2 and CH_4 dissociation in DRM. Herein, the carbon deposition decreases with the increase of the surface adsorbed oxygen species, confirming that the surface oxygen significantly improves resistance in the carbon deposition during DRM. On the other hand, the content of adsorbed oxygen species reflects the concentration of oxygen vacancies on catalyst [55]. Those oxygen vacancies could also promote the adsorption and activation of CO_2, which has already been reported in the literature [20, 24, 57]. Therefore, both aspects can contribute to the lower carbon deposition on the 5Al-5Mn and 2.5Al-7.5Mn catalysts.

The XRD patterns of calcined, reduced, and used Ni-Zr-Al-Mn catalysts are reported in **Figure 6**. The tetragonal ZrO_2 reflections with the crystallite sizes of 9 nm based on the Scherrer equation could be identified for all calcined, reduced, and used catalysts. The peak at about 43.3 ° and 44.5 °can be assigned to the NiO and Ni^0 species [58, 59]. The NiO reflections present on calcined catalysts, disappear on all the reduced catalysts, indicating that the nickel species have been reduced on all the reduced catalysts. As listed in **Table 5**, one can be noted that the existence of both Al and Mn results in a smaller crystalline size of nickel species (both NiO and Ni^0) on all catalysts. The same positive effect was observed for Al and Mn promoted catalysts in literature [60, 61]. The 2.5Al-7.5Mn and 5Al-5Mn catalysts have smaller crystallite sizes of Ni^0 species (<20 nm), which might contribute to their catalytic activity for DRM, because smaller size of nickel species would enhance the activity. Similar results have also been reported by He et al [33]. While it increases to 22, 20, and 27 nm on 5Al, 7.5Al-2.5Mn, and 5Mn catalysts, respectively. Those relatively large crystallite size of metallic nickel can lead to carbon deposition, thereby leading to lower selectivity for DRM and further resulting higher carbon deposition [5, 62, 63]. Especially on 5Al and 5Mn catalysts, the reflection of carbon could be detected on spent 5Al and 5Mn catalysts with the crystallite size of 11 and 12 nm, respectively. Besides, after 5 h DRM activity tests, slight sintering occurred on 2.5Al-7.5Mn catalyst after DRM tests, and the crystallite Ni^0 sizes increased from 16 nm to 18 nm. Thus, the activity of the 2.5Al-7.5Mn catalyst decreased a little with time on stream. While for others, the Ni^0 crystallite sizes of spent catalysts are slightly smaller than those on the reduced catalysts, since the redispersion of Ni species occurs upon continuous reduction and oxidation of nickel [5, 64]. which is in agreement with the results reported by Świrk [15].

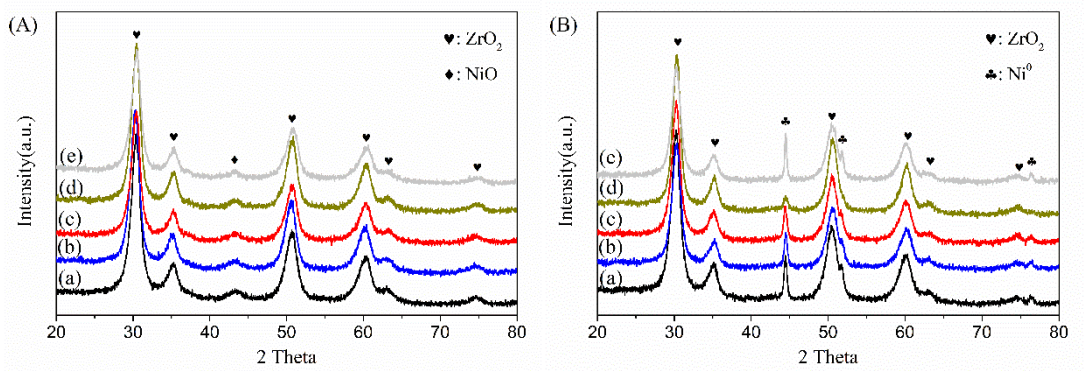

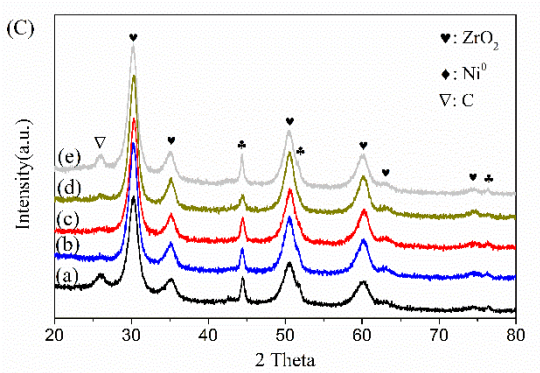

Figure 6 The XRD results of (A) calcinated, (B) reduced and (C) used 5Al (a), 7.5Al-2.5Mn (b), 5Al-5Mn (c), 2.5Al-7.5Mn (d) and 5Mn (e) catalysts.

It implies that the other catalysts could suppress the sintering of nickel-metal during the DRM reaction. The Ni^0 crystallite sizes on 5Al, 7.5Al-2.5Mn, 5Al-5Mn and 5Mn catalysts decreased, while their activity showed different trend during the 5 h DRM. For 7.5Al-2.5Mn catalyst, the activity decreased. For the 5Al and 5Al-5Mn catalysts, the activity did not change. However, the activity on 5Mn catalyst decreased within one hour and then increased. The large particle size of Ni^0 on 5Mn catalyst resulted in carbon deposition, thereby led to partial deactivation. After reaction, the crystallite size of Ni^0 species decreased, while during the reaction process, the activity increased after one hour. Those phenomena mean the nickel redispersion might promote the activity for DRM by the existence of Mn. A similar phenomenon was reported by Li et al. [34].

Table 5 Crystalline sizes of Ni-Zr-Al-Mn catalysts, after reduction at 750 °C for 1 hour and after reaction at 700 °C for 5 hours

	ZrO_2 (nm)			NiO (nm)	Ni^0 (nm)		C (nm)
	calcined	reduced	reaction	calcined	reduced	reaction	reaction
5Al	9	9	9	15	22	19	11
7.5Al-2.5Mn	9	9	9	11	20	18	-
5Al-5Mn	10	10	10	13	19	17	-
2.5Al-7.5Mn	10	10	9	14	16	18	-
5Mn	10	9	10	17	27	20	12

3.4 Discussion

It is well known that large nickel particle size may lead to carbon deposition [62, 63], and the low basic sites also affect the carbon deposition [19, 25]. For the 5Al-5Mn catalyst, both smaller nickel particle size and higher number of basic sites contribute to lower carbon deposition during DRM. More strong basic sites were formed on 5Al and 7.5Al-2.5Mn catalysts, resulting in a higher carbon deposition since strong basic sites would lead to too strong adsorption of CO_2. Similar results were reported in the literature [49]. Besides, the weak and medium-strength basic sites could promote the adsorption and/or activation of CO_2, and further reduce the carbon deposition [2, 49, 50]. It has been also found that the addition of Mn promoter leads to a reduction not only of the formation of coke but also in the rate of the DRM reaction [28, 60, 65], therefore, the 5Mn catalyst exhibited slight lower carbon deposition (lower than 5Al) and lower activity for DRM in the beginning. Besides, the adsorbed oxygen species is inversely proportional to carbon deposition. Higher content of adsorbed oxygen species results in lower carbon deposition. Because adsorbed oxygen species contribute to the adsorption and activation of CO_2, thereby reducing the carbon deposition [31, 54].

4. Conclusions

Al and Mn-promoted Ni catalysts supported on ZrO_2 were synthesized by a one-step synthesis method and tested in DRM at 700 °C with the GSHV of 48,000 h^{-1}. Based on the DRM results, the addition of both Al and Mn promoters could enhance the activity with lower carbon deposition for dry reforming of methane. And the 5Al-5Mn (5 wt% Al and 5 wt% Mn) catalyst exhibited the highest catalytic performance for DRM, as well as the lower carbon deposition. According to the XRD, XPS, and CO_2-TPD characterizations, the results showed more medium-strength basic sites, smaller crystallite size, and higher content of adsorbed oxygen species on the 5Al-5Mn catalyst. All the properties were beneficial for catalyst stability in limiting the carbon deposition. Meanwhile, this work clearly showed that the adsorbed oxygen species was inversely related to carbon deposition. That is the more adsorbed oxygen species, the less carbon deposition.

CRediT authorship contribution statement

Ye: Conceptualization, Investigation, Formal analysis, Writing - original draft, Writing - review &

editing. Li: Investigation, Writing - review & editing. Cui: Investigation, Writing - review & editing. Patrick: Conceptualization, Supervision, Writing - review & editing. Changwei: Conceptualization, Supervision, Writing - review & editing.

Acknowledgments

Ye Wang acknowledges the financial support of CSC (China Scholarship Council) for her joint-PhD research at Sorbonne Université. We thank Yunfei Tian of the analytical & testing center of Sichuan University for XPS experiments.

Funding

This work was supported by the National Key R&D Program of China (2018YFB1501404), the 111 program (B17030), and Fundamental Research Funds for the Central Universities.

Notes

The authors declare no competing financial interest.

References

[1] S. Corthals, J. V. Nederkassel, H. D.Winne, Design of active and stable $NiCeO_2ZrO_2MgAl_2O_4$ dry reforming catalysts, Appl. Catal. B: Environ. 105 (2011) 263-275.

[2] Y. Wang, L. Yao, S. Wang, D. Mao, C. Hu, Low-temperature catalytic CO_2 dry reforming of methane on Ni-based catalysts: a review, Fuel Process. Technol. 169 (2018) 199-206.

[3] E. Ryckebosch, M. Drouillon, H. Vervaeren, Techniques for transformation of biogas to biomethane, Biomass Bioenerg. 35 (2011) 1633-1645.

[4] A. Djaidja, S. Libs, A. Kiennemann, A. Barama, Characterization and activity in dry reforming of methane on NiMg/Al and Ni/MgO catalysts, Catal. Today, 113 (2006) 194-200.

[5] Y. Wang, L. Li, Y. Wang, P. Da Costa, C. Hu, Highly Carbon-Resistant Y Doped NiO–ZrO_m Catalysts for Dry Reforming of Methane, Catalysts, 9 (2019) 1055.

[6] C. Wang, N. Sun, N. Zhao, W. Wei, Y. Zhao, Template-free preparation of bimetallic mesoporous Ni-Co-CaO-ZrO_2 catalysts and their synergetic effect in dry reforming of methane, Catal. Today, 281 (2017) 268-275.

[7] J. Titus, T. Roussiere, G. Wasserschaff, S. Schunk, A. Milanov, E. Schwab, G. Wagner, O. Oeckler, R. Gläser, Dry reforming of methane with carbon dioxide over NiO–MgO–ZrO_2, Catal. Today, 270 (2016) 68-75.

[8] A. Ochoa, A. Arregi, M. Amutio, A.G. Gayubo, M. Olazar, J. Bilbao, P. Castaño, Coking and sintering progress of a Ni supported catalyst in the steam reforming of biomass pyrolysis volatiles, Appl. Catal. B: Environ. 233 (2018) 289-300.

[9] Q. Zhang, T. Zhang, Y. Shi, B. Zhao, M. Wang, Q. Liu, J. Wang, K. Long, Y. Duan, P. Ning, A sintering and carbon-resistant Ni-SBA-15 catalyst prepared by solid-state grinding method for dry reforming of methane, J. CO_2 Util. 17 (2017) 10-19.

[10] Y. Lou, M. Steib, Q. Zhang, K. Tiefenbacher, A. Horváth, A. Jentys, Y. Liu, J.A. Lercher, Design of stable Ni/ZrO_2 catalysts for dry reforming of methane, J. Catal. 356 (2017) 147-156.

[11] Q. Chen, J. Zhang, B. Pan, W. Kong, Y. Chen, W. Zhang, Y. Sun, Temperature-dependent anti-coking behaviors of highly stable Ni-CaO-ZrO_2 nanocomposite catalysts for CO_2 reforming of methane, Chem. Eng. J. 320 (2017) 63-73.

[12] J. Won-Jun, S. Jae-Oh, K. Hak-Min, Y. Seong-Yeun, R. Hyun-Seog, A review on dry reforming of methane in aspect of catalytic properties, Catal. Today, 324 (2019) 15-26.

[13] K. Mette, S. Kühl, A. Tarasov, H. Düdder, K. Kähler, M. Muhler, R. Schlögl, M. Behrens, Redox dynamics of Ni catalysts in CO_2 reforming of methane, Catal. Today, 242 (2015) 101-110.

[14] L.A. Arkatova, The deposition of coke during carbon dioxide reforming of methane over intermetallides, Catal. Today, 157 (2010) 170-176.

[15] K. Świrk, M.E. Galvez, M. Motak, T. Grzybek, M. Rønning, P. Da Costa, Dry reforming of methane over Zr-and Y-modified Ni/Mg/Al double-layered hydroxides, Catal. Commun. 117 (2018) 26-32.

[16] M. Miyamoto, A. Hamajima, Y. Oumi, S. Uemiya, Effect of basicity of metal doped ZrO_2 supports on hydrogen production reactions, Int. J. Hydrogen Energ. 43 (2018) 730-738.

[17] S.M. Sajjadi, M. Haghighi, F. Rahmani, Sol–gel synthesis of Ni–Co/Al_2O_3–MgO–ZrO_2 nanocatalyst used in hydrogen production via reforming of CH_4/CO_2 greenhouse gases, J. Nat. Gas Sci. Eng. 22 (2015) 9-21.

[18] L. Yao, J. Shi, H. Xu, W. Shen, C. Hu, Low-temperature CO_2 reforming of methane on Zr-promoted Ni/SiO_2 catalyst, Fuel Process. Technol. 144 (2016) 1-7.

[19] X. Zhao, Y. Cao, H. Li, J. Zhang, L. Shi, D. Zhang, Sc promoted and aerogel confined Ni catalysts for coking-resistant dry reforming of methane, RSC Adv. 7 (2017) 4735-4745.

[20] Y.J. Asencios, C.B. Rodella, E.M. Assaf, Oxidative reforming of model biogas over NiO–Y_2O_3–ZrO_2 catalysts, Appl. Catal. B: Environ. 132 (2013) 1-12.

[21] B. Koubaissy, A. Pietraszek, A. Roger, A. Kiennemann, CO_2 reforming of methane over Ce-Zr-Ni-Me mixed catalysts, Catal. Today, 157 (2010) 436-439.

[22] F. Pompeo, N.N. Nichio, O.A. Ferretti, D. Resasco, Study of Ni catalysts on different supports to obtain synthesis gas, Int. J. Hydrogen Energ. 30 (2005) 1399-1405.

[23] N. Wang, W. Chu, T. Zhang, X.-S. Zhao, Manganese promoting effects on the Co–Ce–Zr–O_x nano catalysts for methane dry reforming with carbon dioxide to hydrogen and carbon monoxide, Chem. Eng. J. 170 (2011) 457-463.

[24] J.D. Bellido, E.M. Assaf, Effect of the Y_2O_3–ZrO_2 support composition on nickel catalyst evaluated in dry reforming of methane, Appl. Catal. A: Gen. 352 (2009) 179-187.

[25] H. Liu, H.B. Hadjltaief, M. Benzina, M.E. Gálvez, P. Da Costa, Natural clay based nickel catalysts for dry reforming of methane: On the effect of support promotion (La, Al, Mn), Int. J. Hydrogen Energ. 44 (2019) 246-255.

[26] S.K. Talkhoncheh, M. Haghighi, Syngas production via dry reforming of methane over Ni-based nanocatalyst over various supports of clinoptilolite, ceria and alumina, J. Nat. Gas Sci. Eng. 23 (2015) 16-25.

[27] A.E.C. Luna, M.E. Iriarte, Carbon dioxide reforming of methane over a metal modified Ni-Al_2O_3 catalyst, Appl. Catal. A: Gen. 343 (2008) 10-15.

[28] Y. Lu, J. Zhu, X. Peng, D. Tong, C. Hu, Comparative study on the promotion effect of Mn and Zr on the stability of Ni/SiO_2 catalyst for CO_2 reforming of methane, Int. J. Hydrogen Energ. 38 (2013) 7268-7279.

[29] S.-H. Seok, S.H. Choi, E.D. Park, S.H. Han, J.S. Lee, Mn-promoted Ni/Al_2O_3 catalysts for stable carbon dioxide reforming of methane, J. Catal. 209 (2002) 6-15.

[30] C. Li, P.-J. Tan, X.-D. Li, Y.-L. Du, Z.-H. Gao, W. Huang, Effect of the addition of Ce and Zr on the structure and performances of Ni–Mo/CeZr–MgAl(O) catalysts for CH_4–CO_2 reforming, Fuel Process. Technol. 140 (2015) 39-45.

[31] Y. Wang, Q. Zhao, Y. Wang, C. Hu, P. Da Costa, One-step synthesis of highly active and

stable Ni-ZrO_x for dry reforming of methane, Ind. Eng. Chem. Res. 59 (2020) 11441–11452.

[32] W. Li, X. Jie, C. Wang, J.R. Dilworth, C. Xu, T. Xiao, P.P. Edwards, MnO_x-Promoted, Coking-Resistant Nickel-based Catalysts for Microwave-initiated CO_2 Utilization, Ind. Eng. Chem. Res. 59 (2020) 6914–6923

[33] S. He, H. Wu, W. Yu, L. Mo, H. Lou, X. Zheng, Combination of CO_2 reforming and partial oxidation of methane to produce syngas over Ni/SiO_2 and Ni–Al_2O_3/SiO_2 catalysts with different precursors, Int. J. Hydrogen Energ. 34 (2009) 839-843.

[34] X. Li, J.S. Chang, M. Tian, S.E. Park, CO_2 reforming of methane over modified Ni/ZrO_2 catalysts, Appl. Organomet. Chem. 15 (2001) 109-112.

[35] Y. Wang, L. Yao, Y. Wang, S. Wang, Q. Zhao, D. Mao, C. Hu, Low-temperature catalytic CO_2 dry reforming of methane on Ni-Si/ZrO_2 catalyst, ACS Catal. 8 (2018) 6495-6506.

[36] M.K. Nikoo, N. Amin, Thermodynamic analysis of carbon dioxide reforming of methane in view of solid carbon formation, Fuel Process. Technol. 92 (2011) 678-691.

[37] M.M. Souza, D.A. Aranda, M. Schmal, Reforming of methane with carbon dioxide over Pt/ZrO_2/Al_2O_3 catalysts, J. Catal. 204 (2001) 498-511.

[38] J. Rostrupnielsen, J.B. Hansen, CO_2-reforming of methane over transition metals, J. Catal. 144 (1993) 38-49.

[39] Ş. Özkara-Aydınoğlu, A.E. Aksoylu, Carbon dioxide reforming of methane over Co-X/ZrO_2 catalysts (X= La, Ce, Mn, Mg, K), Catal. Commun. 11 (2010) 1165-1170.

[40] K. Świrk, M.E. Galvez, M. Motak, T. Grzybek, M. Rønning, P. Da Costa, Yttrium promoted Ni-based double-layered hydroxides for dry methane reforming, J. CO_2 Util. 27 (2018) 247-258.

[41] T. Bai, X. Zhang, F. Wang, W. Qu, X. Liu, C. Duan, Coking behaviors and kinetics on HZSM-5/SAPO-34 catalysts for conversion of ethanol to propylene, J. Energ. Chem. 25 (2016) 545-552.

[42] A.R. McFarlane, I.P. Silverwood, E.L. Norris, R.M. Ormerod, C.D. Frost, S.F. Parker, D. Lennon, The application of inelastic neutron scattering to investigate the steam reforming of methane over an alumina-supported nickel catalyst, Chem. Phys. 427 (2013) 54-60.

[43] A. Sadezky, H. Muckenhuber, H. Grothe, R. Niessner, U. Pöschl, Raman microspectroscopy of soot and related carbonaceous materials: Spectral analysis and structural information, Carbon, 43 (2005) 1731-1742. 22 (2015) 9-21

[44] S.A. Chernyak, A.S. Ivanov, K.I. Maslakov, A.V. Egorov, Z. Shen, S.S. Savilov, V.V. Lunin, Oxidation, defunctionalization and catalyst life cycle of carbon nanotubes: a Raman spectroscopy view, Phys. Chem. Chem. Phys. 19 (2017) 2276.

[45] H. Liu, D. Wierzbicki, R. Debek, M. Motak, T. Grzybek, P.D. Costa, M.E. Gálvez, La-promoted Ni-hydrotalcite-derived catalysts for dry reforming of methane at low temperatures, Fuel, 182 (2016) 8-16.

[46] R. Dębek, M.E. Galvez, F. Launay, M. Motak, T. Grzybek, P. Da Costa, Low temperature dry methane reforming over Ce, Zr and CeZr promoted Ni–Mg–Al hydrotalcite-derived catalysts, Int. J. Hydrogen Energ. 41 (2016) 11616-11623.

[47] V. García, J.J. Fernández, W. Ruíz, F. Mondragón, A. Moreno, Effect of MgO addition on the basicity of Ni/ZrO_2 and on its catalytic activity in carbon dioxide reforming of methane, Catal. Commun. 11 (2009) 240-246.

[48] X. Zhang, Q. Zhang, N. Tsubaki, Y. Tan, Y. Han, Carbon dioxide reforming of methane over Ni nanoparticles incorporated into mesoporous amorphous ZrO_2 matrix, Fuel, 147 (2015) 243-252.

[49] R. Dębek, M. Motak, M.E. Galvez, T. Grzybek, P. Da Costa, Influence of Ce/Zr molar ratio on catalytic performance of hydrotalcite-derived catalysts at low temperature CO_2 methane reforming, Int. J. Hydrogen Energ. 42 (2017) 23556-23567.

[50] R. Dębek, M. Motak, M.E. Galvez, P. Da Costa, T. Grzybek, Catalytic activity of hydrotalcite-derived catalysts in the dry reforming of methane: on the effect of Ce promotion and feed gas composition, React. Kinet. Mech. Cat. 121 (2017) 185-208.

[51] Y. Xu, H. Long, Q. Wei, X. Zhang, S. Shang, X. Dai, Y. Yin, Study of stability of Ni/MgO/γ-Al_2O_3 catalyst prepared by plasma for CO_2 reforming of CH_4, Catal. Today, 211 (2013) 114–119.

[52] A. F. Al-Fastesh, R. Kumar, S. O. Kasim, A .A .Ibrahim, A. H. Fakeeha, A. E. Abasaeed, R. Alrasheed, A. Bagabas, M. L. Chaudary, F. Frusteri, B. Chowdhury, The effect of modifier identity on the performance of Ni-based catalyst supported on γ-Al_2O_3 in dry reforming of methane, Catal. Today, 348 (2020) 236-242.

[53] R. Dębek, M. Motak, D. Duraczyska, F. Launay, M.E. Galvez, T. Grzybek, P. Da Costa, Methane dry reforming over hydrotalcite-derived Ni–Mg–Al mixed oxides: the influence of Ni

content on catalytic activity, selectivity and stability, Catal. Sci. Technol. 6 (2016) 6705-6715.

[54] M. Zhang, J. Zhang, Y. Wu, J. Pan, Q. Zhang, Y. Tan, Y. Han, Insight into the effects of the oxygen species over Ni/ZrO_2 catalyst surface on methane reforming with carbon dioxide, Appl. Catal. B: Environ. 244 (2019) 427-437.

[55] H. Wang, J. Liu, Z. Zhao, Y. Wei, C. Xu, Comparative study of nanometric Co-, Mn- and Fe-based perovskite-type complex oxide catalysts for the simultaneous elimination of soot and NO_x from diesel engine exhaust, Catal. Today, 184 (2012) 288-300.

[56] H. Liang, Y. Hong, C. Zhu, S. Li, Y. Chen, Z. Liu, D. Ye, Influence of partial Mn-substitution on surface oxygen species of $LaCoO_3$ catalysts, Catal. Today, 201 (2013) 98-102.

[57] Y.J.O. Asencios, F.C.F. Marcos, J.M. Assaf, E.M. Assaf, Oxidative-reforming of methane and partial oxidation of methane reaction over NiO/PrO_2/ZrO_2 catalysts: effect of the nickel content, Braz. J. Chem. Eng. 33 (2016) 627-636.

[58] L. Yao, Y. Wang, J. Shi, H. Xu, W. Shen, C. Hu, The influence of reduction temperature on the performance of ZrO_x/Ni-MnO_x/SiO_2 catalyst for low-temperature CO_2 reforming of methane, Catal. Today, 281 (2017) 259-267.

[59] Z. Miao, Z. Li, C. Suo, J. Zhao, W. Si, J. Zhou, S. Zhuo, One-pot synthesis of Al_2O_3 modified mesoporous ZrO_2 with excellent thermal stability and controllable crystalline phase, Adv. Powder Technol. 29 (2018) 3569-3576.

[60] F. Guo, J.-Q. Xu, W. Chu, CO_2 reforming of methane over Mn promoted Ni/Al_2O_3 catalyst treated by N_2 glow discharge plasma, Catal. Today, 256 (2015) 124-129.

[61] X. Liu, J. Toyir, P. Ramirez de la Piscina, N. Homs, Hydrogen production from methanol steam reforming over Al_2O_3- and ZrO_2-modified CuOZnOGa_2O_3 catalysts, Int. J. Hydrogen Energ. 42 (2017) 13704-13711.

[62] K. Świrk, M.E. Gálvez, M. Motak, T. Grzybek, M. Rønning, P. Da Costa, Syngas production from dry methane reforming over yttrium-promoted nickel-KIT-6 catalysts, Int. J. Hydrogen Energ. 44 (2019) 274-286.

[63] K. Sutthiumporn, S. Kawi, Promotional effect of alkaline earth over Ni–La_2O_3 catalyst for CO_2 reforming of CH_4: role of surface oxygen species on H_2 production and carbon suppression, Int. J. Hydrogen Energ. 36 (2011) 14435-14446.

[64] T. Nakayama, M. Arai, Y. Nishiyama, Dispersion of nickel particles supported on alumina

and silica in oxygen and hydrogen, J. Catal. 87 (1984) 108-115.

[65] T. Osaki, T. Mori, Role of potassium in carbon-free CO_2 reforming of methane on K-promoted Ni/Al_2O_3 catalysts, J. Catal. 204 (2001) 89-97